ELSEVIER

Polymer 40 (1999) 6965–6975

polymer

Morphology-interface-toughness relationship in polyamide/polysulfone blends by reactive processing

P. Charoensirisomboon[a], T. Chiba[a], K. Torikai[a], H. Saito[a], T. Ougizawa[a], T. Inoue[a,*], M. Weber[b]

[a]*Department of Organic and Polymeric Materials, Tokyo Institute of Technology, Ookayama Meguro-ku, Tokyo 152-8552, Japan*
[b]*BASF, Polymer Research Laboratory, D-67056 Ludwigshafen, Germany*

Received 28 October 1998; received in revised form 14 December 1998; accepted 24 December 1998

Abstract

By reactive blending of polyamide 6 (PA) with polysulfone (PSU) using a gram-scale mixer (Mini–Max Molder), we prepared a series of PA/PSU (80/20 wt. ratio) blends with various diameters of PSU particles; 70 nm by using phthalic anhydride-terminated PSU (PSU-PhAH), 0.4 μm by epoxy-terminated PSU, 0.45 μm by maleic anhydride-grafted PSU and 1.3 μm by non-reactive PSU. By light scattering (LS), small-angle X-ray scattering (SAXS), wide-angle X-ray diffraction (WAXD), and differential scanning calorimetry, it was shown that there did not exist any difference in the crystalline morphology of PA matrix among the blends. Although difference in tensile strength among blends was small but on elongation it was large; the smaller PSU particles yielded larger elongation at break. The bulk-fracture toughness was shown to be higher for the blend with smaller PSU particles. Especially, PSU-PhAH blend showed a remarkably high toughness. In this blend, ductile fracture was shown by SEM observation. Transmission electron microscopic (TEM) observation confirmed the homogenous plastic deformation without interfacial debonding in the two-phase material. In contrast, other blends showed brittle fracture accompanied with interfacial debonding. The adhesive strength between PA and PSU-PhAH phases measured by asymmetric double cantilever beam method was shown to be much higher than in other systems. Thus, when the interfacial adhesive strength is high enough to provide adequate stress transfer, plastic deformation of brittle PSU particle can occur and hence the uniform plastic deformation of the whole material may render high toughness. The lower interfacial adhesion seems to yield in less massive plastic deformation to resulting in lower toughness.

Keywords: Polymer blends; Reactive blending; Toughness

1. Introduction

Rubber-toughened plastics, such as polyamide (PA)/rubber, polycarbonate (PC)/poly (butylene terephthalate) (PBT)/rubber and PC/PBT/ABS, are binary or ternary alloys, in which fine rubber particles are dispersed in ductile matrices. Wu [1,2] investigated the toughening mechanism of PA/rubber system to show that the impact energy dissipation is achieved mostly by homogeneous yielding of the PA matrix. Borggreve et al. [3], Hobbs and Dekkers [4] and Sue and Yee [5] suggested another toughening mechanism for the PPO/PA/rubber system. They proposed the importance of rubber cavitation: either cavitation or void formation within the rubber particles or the interface plays an important role in the toughening process. By elastic–plastic analysis of deformation mechanism, Fukui et al. [6] showed that the two mechanisms are not conflicting: a massive yielding of matrix occurs by bulk deformation and then, even after the cavitation or the debonding takes place, the yielding can still proceed to dissipate more energy.

It is also known that ductile polymers, e.g. PA and PC can be toughened by blending with brittle polymer such as poly (methyl methacrylate) (PMMA), poly (styrene-co-acrylonitril) (SAN) [7,8]. The toughening mechanism is interpreted by "cold-drawing concept": the impact energy is absorbed by a large plastic deformation of the brittle particles in a ductile matrix. Angola et al. [9] found a significant increase in impact toughness of PA matrix with brittle dispersed SAN when small amount of the third component, poly(styrene-co-maleic anhydride) (SMA) was added as a reactive interfacial compatibilizer. A good interfacial adhesion between the ductile matrix and the brittle particles seems to be a prerequisite for suitable stress transfer to induce cold drawing. More recently, Liu et al. [10] and Evan et al. [11] showed similar results in linear low-density polyethylene/PMMA and high-density polyethylene/polystyrene blends when the reactive interfacial compatibilization was applied.

* Corresponding author. Tel.: +81 3 5734 2439; fax: +81 3 5734 2876.
E-mail address: tinoue@o.cc.titech.ac.jp (T. Inoue)

0032-3861/99/$ - see front matter © 1999 Elsevier Science Ltd. All rights reserved.
PII: S0032-3861(99)00011-7

nf-PSU

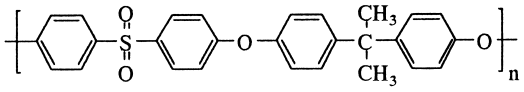

PSU-epoxy

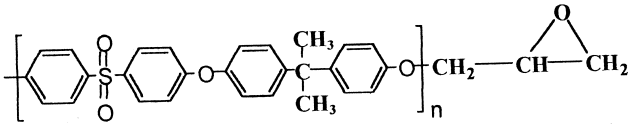

PSU-PhAH

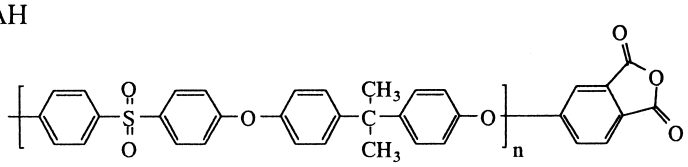

PSU-MAH

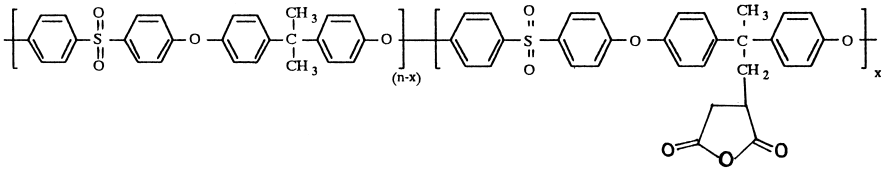

Fig. 1. Chemical structures of synthesized polysulfones.

We recently carried out reactive blending of PA6 with polysulfone (PSU) and found that one can control PSU particle size in a wide range, 1~40 nm, by using various functional groups attached to PSU chains such as epoxide, maleic anhydride and phthalic anhydride [12,13]. The functionalized PSU samples had low molecular weight (M_n~5000) so that they were brittle. Then, the PA/PSU systems give a nice opportunity for extending the study on toughening mechanism of brittle/ductile tough blends. In this study, melt blending of the functionalized PSU with PA was carried out at 20/80 (PSU/PA) wt. ratio in a one-gram scale mixer. Mechanical properties were measured under both plane-stress and more plane-strain condition by using a thin film (0.3 mm) and a notched thick specimen (1.5 mm), respectively. We carefully investigated the effect of PSU particle size on crystalline morphology of PA matrix by wide angle X-ray diffraction (WAXD), small-angle X-ray scattering (SAXS) and light scattering (LS), i.e. in a length scale from nm to μm. Moreover, investigation was also extended to the interfacial adhesive strength between PA and PSU phases by asymmetric double cantilever beam method. We then discuss the morphology-interface-toughness relationship in the ductile/brittle blends.

2. Theoretical background

The cold drawing of brittle polymer particle in ductile polymer matrix has been shown to be a rather general phenomenon for a class of brittle/ductile combination [7,14]. The cold drawing takes place by triaxial stress concentrations caused by bulk deformation of the two-phase materials, provided that adequate differences in Young's modulus and Poisson's ratio exist between the particles and the matrix. Following the von Mises's criterion for yielding, homogenous yielding can occur if

$$(\sigma_x - \sigma_y)^2 + (\sigma_y - \sigma_z)^2 + (\sigma_z - \sigma_x)^2 \geq 6k^2, \quad (1)$$

where σ_x, σ_y, and σ_z are the three principal stresses, and k is a material constant. The von Mises's criterion in Eq. (1) means that yielding will occur when the shear strain energy density reaches a critical value. The three principal stresses evolved by the bulk deformation are calculated, e.g. by the

Table 1
Characteristics of polymers

Code	M_n[a]	M_w[a]	Viscosity no.[b]	Functionality[c]
PA	13 000	25 000		
nf-PSU	5 700	28 800	36.2	
PSU-MAH	9 250	27 130	34.3	1.36
PSU-epoxy	6 970	20 010	27	0.25
PSU-PhAH	5 310	20 660	29	1.25

[a] GPC measurement, g/mol.
[b] Solution viscosity, ml/g.
[c] Content of functional group, wt. %.

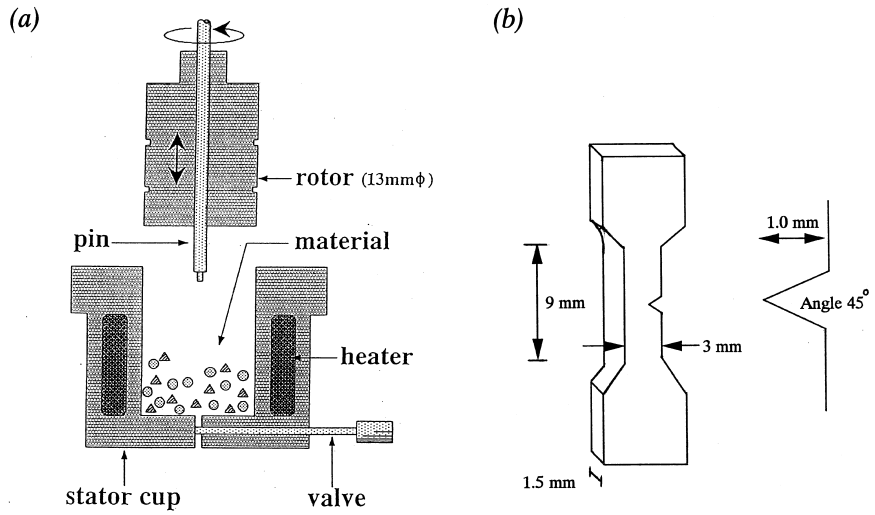

Fig. 2. (a) Mini–Max Molder and (b) dimension of notched dumbbell specimen.

Goodier's equation and the modified Eshelby's equation [9,14]. Then, the toughening by cold drawing of SAN particles in PC, PA and PBT matrices was successfully interpreted. Also interpreted was the failure of cold drawing in PS/PC and PS/PA systems [14].

The aforementioned discussion is on the basis of the implicit assumption of perfect interfacial adhesion between the particle and the matrix, i.e., infinitely strong interface. There is no interfacial problem in the direction perpendicular to the stretching direction, because the stress evolved is a compressive one. However, the stress evolved in the stretching direction is an elongational one and its magnitude is usually high. So, if the adhesive strength was low, debonding would take place before the particles are subjected to high stress concentration necessary for yielding. If the adhesive strength is enhanced, e.g. by in situ formed block or graft copolymers at interface, proper stress transfer is expected to induce the brittle–ductile transition, and the two-phase system should be toughened.

Another point to be discussed is the effect of particle size. By in situ formation of block or graft copolymers, the particle size is usually reduced. The argument by stress analysis by Eq. (1) may be valid no matter how big or small is the particle size. However, the particle size should affect the crystalline morphology of matrix, when the matrix polymer is crystalline polymer such as PA and PBT [19]. So the mechanical properties of matrix might depend on the particle size. In such case, the situation becomes very complicated so that one cannot discuss the cold drawing simply by Eq. (1). To investigate the effect of interfacial strength on cold drawing, for example, the mechanical property of matrix should be kept constant.

PA/PSU systems would provide a nice opportunity to get a better understanding on the toughening mechanism by cold drawing, provided the interfacial adhesive strength between PA and PSU phases could be estimated, the crystalline morphology of PA matrix could be carefully investigated, and the cold drawing of PSU could be clearly justified.

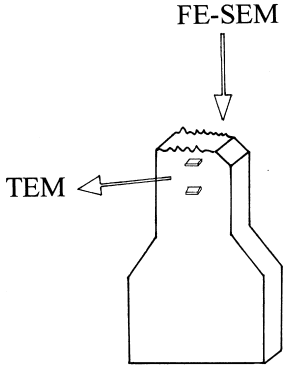

Fig. 3. Electron microscopic views of fractured dumbbell specimen.

3. Experimental section

3.1. Materials

PA used was a commercial PA6 (Ultramid B3, BASF). PSU without functional group (nf-PSU) and three different types of functionalized PSU were prepared by following the synthesis procedures given in the literature [15–17]. The details of the synthesis method is reported elsewhere [12,13]. The chemical structures of PSU used are shown in Fig. 1 and the characteristics of the materials used are summarized in Table 1.

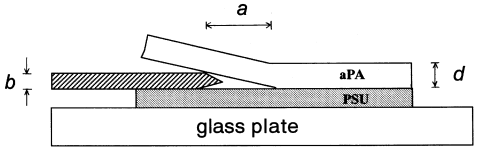

Fig. 4. Schematic representation of welded specimen for the asymmetric double cantilever beam method.

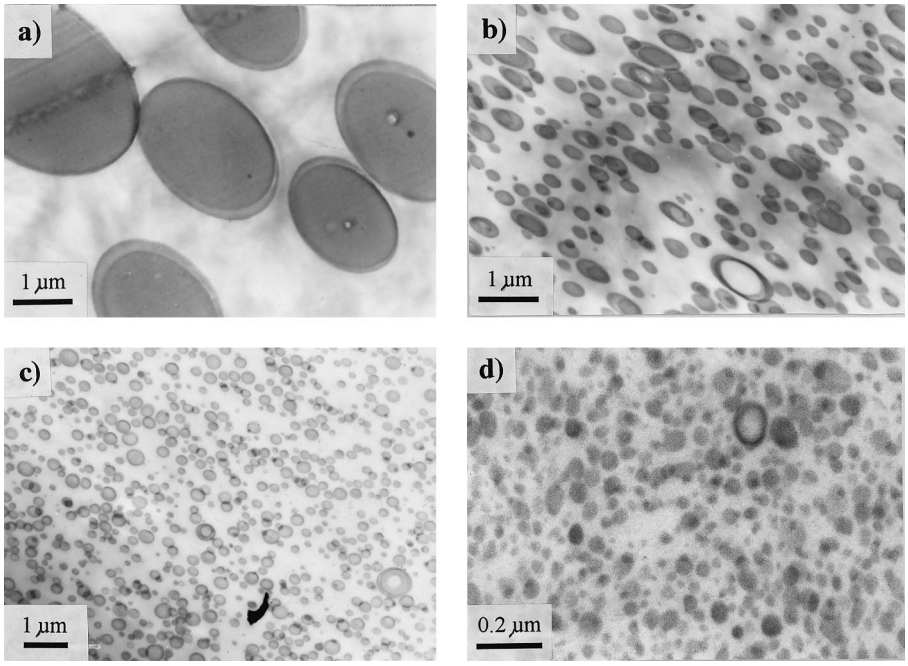

Fig. 5. TEM micrographs (RuO_4 stained) of 80/20 PA/PSU blends melt-mixed at 260°C for 6 min: (a) PA/nf-PSU; (b) PA/PSU-MAH; (c) PA/PSU-epoxy; and (d) PA/PSU-PhAH.

3.2. Sample preparation

PA pellets were dried under vacuum (10^{-4} mmHg) at 80°C for 12 h before mixing to remove water. PA and PSU were melt-mixed in a miniature mixer of one gram-scale, Mini–Max Molder (CS-183 MM, Custom Scientific Instruments) (Fig. 2(a)) at 260°C for 6 min setting rotor speed at 100 rpm. Weight ratio of PSU/PA was fixed at 20/80. The melt-blended polymers were injected into a mold, which had been preheated by a contact with the hot stator cup. After injection, the mold was subsequently removed and immediately quenched in cool water. The mold was designed to deliver a dumbbell specimen. The molded specimen was then notched as shown in Fig. 2(b). The notched specimens were dried under vacuum at room temperature for 48 h before mechanical test.

Thin film specimens were also prepared. The melt-blended materials by Mini–Max Molder was extruded and chopped into pellets. The pellets were then compression-molded between polyimide sheets at 260°C for 1.5 min to prepare film specimens (ca. 0.3 mm thick). Then, the film specimen was quickly quenched in cool water. The specimen was then cut into strips (5 mm × 50 mm) at 70°C (above T_g of PA) in order to avoid crack formation at the film edge. The thin film specimens were also dried under vacuum at room temperature for 48 h before the tensile test.

3.3. Morphology characterization

To observe the morphology, a small amount of the melt-blended polymer was picked up by pincette after 6 min mixing and quenched quickly in cool water. The specimen was cryomicrotomed at −40°C by ultramicrotome (Reichert ultracut-Nissei). The ultrathin section of ca. 60 nm thickness

Table 2
Morphology parameters and interfacial adhesion

Code	D_{TEM}[a] (μm)	X_c[b] (%)	T_m[c] (°C)	ξ_1[d] (μm)	ξ_2[e] (nm)	G_c[f] (Jm^{-2})
PA/nf-PSU	1.3	25.1	220.8	0.34	4.0	~0
PA/PSU-MAH	0.45	26.0	220.7	0.32	3.8	35
PA/PSU-epoxy	0.40	26.2	220.6	0.33	3.8	27
PA/PSU-PhAH	0.07	24.0	220.3	0.36	4.1	110

[a] Mean diameter of PSU particle from TEM micrographs.
[b] Melting temperature of PA by DSC (T_m of PA = 221°C).
[c] Crystallinity by DSC.
[d] Orientation correlation length from LS.
[e] Correlation length in density fluctuation from SAXS.
[f] Fracture Toughness by ADCB.

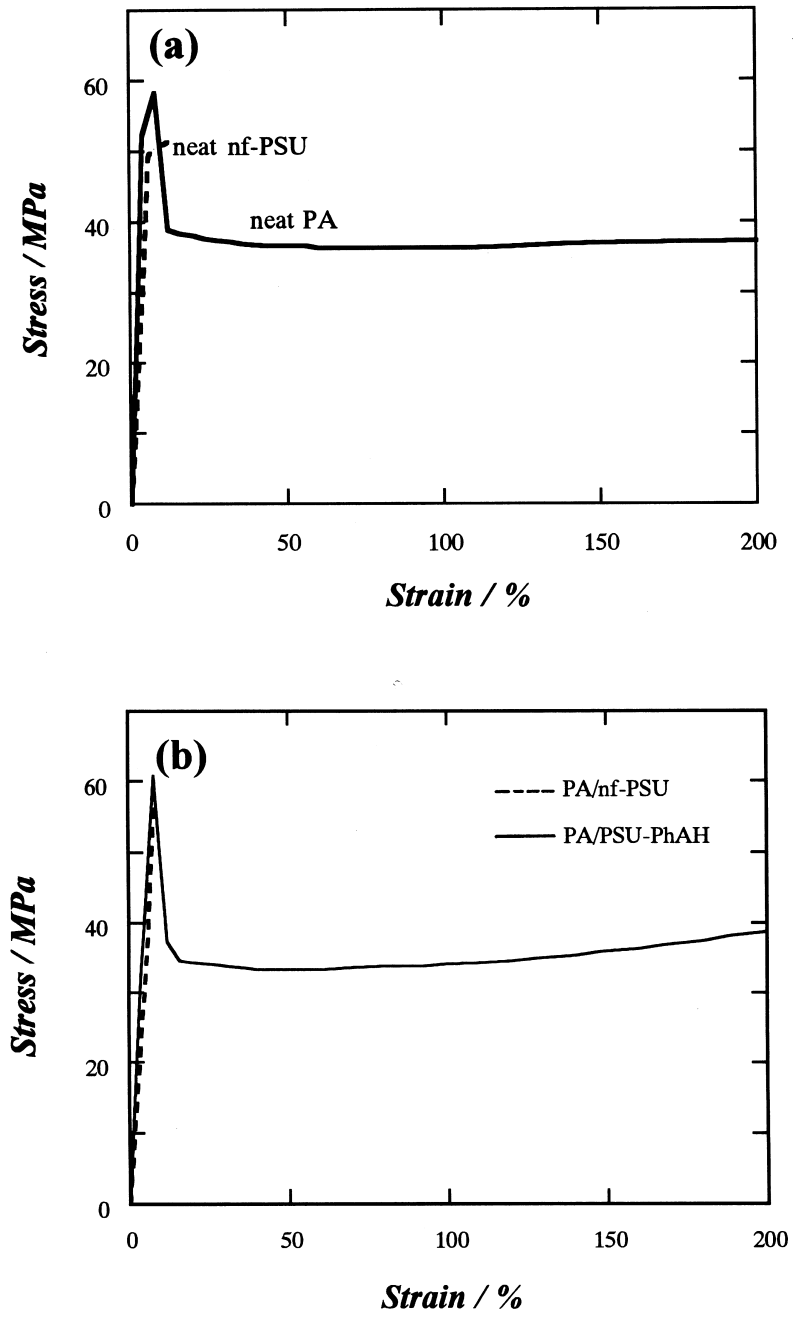

Fig. 6. Stress–strain curves of (a) neat PA and neat nf-PSU and (b) PA/nf-PSU and PA/PSU-PhAH blends.

was mounted on 200 mesh copper grid and exposed to the vapor of ruthenium tetroxide (RuO_4) above a 0.5 wt.% aqueous solution of RuO_4 for 10 min. RuO_4 preferentially stains PSU phase to provide a nice contrast under transmission electron microscopy (TEM). The two-phase morphology was observed by TEM, JEM-100CX (JEOL), at an accelerating voltage of 100 kV. TEM picture was digitized using a scanner (EPSON GT8500). The area of an individual particle a_i was directly determined using a software (NIH Image Analysis System). The diameter of dispersed particles D_i was calculated by $D_i = 2(a_i/\pi)^{1/2}$, assuming that the shape of particle is circular. The average diameter was then obtained by the following equation:

$$D_{\mathrm{TEM}} = \sum_{i=1}^{N} D_i^3 / \sum_{i=1}^{N} D_i^2, \tag{3}$$

where N was 200–500 in a TEM picture.

Crystalline morphology of PA matrix was investigated by WAXD and SAXS using Rigaku Denki RU-200 apparatus. The radiation from Cu anode was reflected from a graphite monochromator to obtain monochromatic CuKα radiation

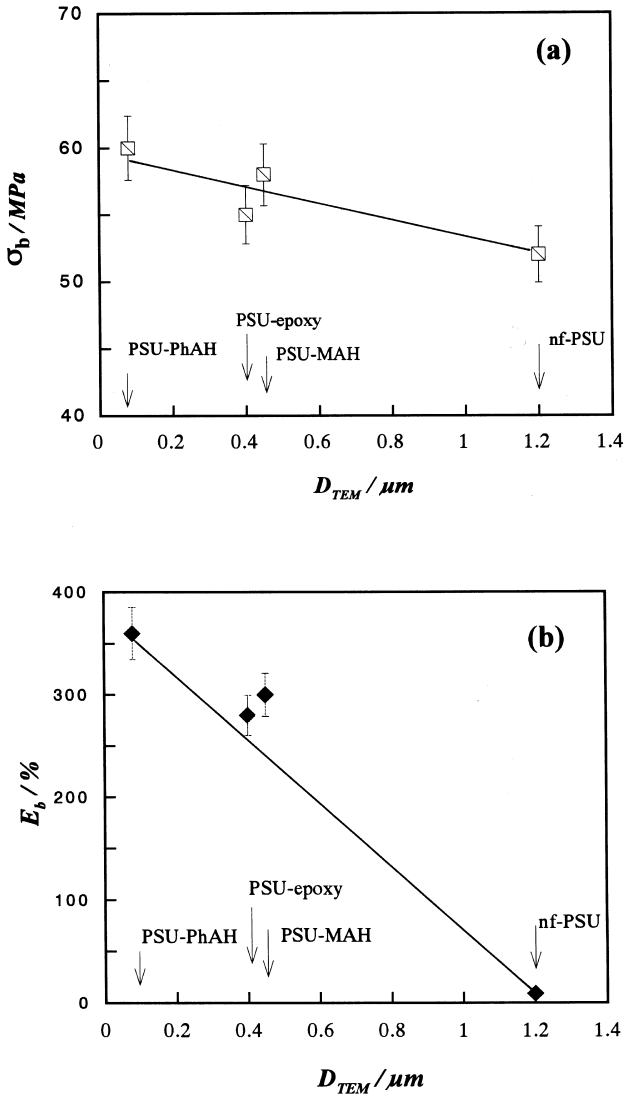

Fig. 7. Mean diameters of dispersed PSU (D_{TEM}) vs. mechanical properties: tensile strength σ_b and elongation at break E_b.

with a wavelength of 0.1541 nm. The generator was operated at 50 kV and 180 mA. The measurements were performed at room temperature.

Crystalline morphology was also characterized by LS in terms of the orientation correlation length, which describes the degree of correlation in orientation of crystallites. To estimate the orientation correlation length, the angular distribution of scattering light at an azimuthal angle μ=45° was measured under H_v geometry (cross polarized condition: optical axis of analyzer and polarizer are perpendicular) by using a highly sensitive CCD (charge-couple device) camera with 576 × 382 pixels in a sensor of 13.3 × 8.8 mm^2 (Princeton Instruments). The details of this apparatus has been reported elsewhere [18,19].

In a differential scanning calorimeter, Seiko EXSTRAR600, neat PA or blend specimen packed in aluminum pan was heated at a heating rate of 10°C min^{-1} under nitrogen atmosphere. The melting temperature and enthalpy of fusion were obtained from the maximum and the area of the endothermic peak, respectively. The relative crystallinity X_c was calculated by $X_c = \Delta H^*/\Delta H^\circ_{PA6}$, where ΔH^* is the enthalpy of fusion per gram of PA or in the blend and ΔH°_{PA6} is the enthalpy of fusion per gram of 100% crystalline PA (230 J/g) [20].

3.4. Mechanical test

A stress–strain curve of the film specimen was measured using a tensile testing machine (Tensilon UTM-II-20, Toyo Baldwin) at constant strain rate of 40 mm min^{-1} at room temperature. A load-displacement curve of the notched specimen was measured at strain rate of 8 and 2 mm min^{-1} using the same tensile testing machine. Note that the test condition was mainly followed ASTM but there were several modifications in specimen dimension.

3.5. Electron microscopy observation of deformed specimen

The fractured surface of notched specimen after testing (Fig. 3) was observed with FE-SEM (Field Emission Scanning Electron Microscope, Model S-800, Hitachi) at an accelerating voltage of 10–15 kV.

The deformed zone was observed by TEM. The fractured specimen was partially embedded in an epoxy resin that was then cured at 40°C. The embedded specimen was trimmed and microtomed in a direction parallel to the fractured plane as shown in Fig. 3. It was then was stained by RuO_4 and observed under TEM as described earlier.

3.6. Adhesion test

Adhesive strength between the PA and PSU phases was estimated by asymmetric double cantilever beam method (ADCB) in terms of the fracture toughness, G_c [21,22]. Sample for ADCB having geometry shown in Fig. 4 was prepared as follows. First, the amorphous polyamide (aPA)[1] and nf-PSU substrates were prepared by melt-press at 200°C and 240°C, respectively. Then, the substrates were cut to a strip of 5.0 cm × 1.0 cm × 0.3 cm. Second, a thin functionalized PSU film of ca. 0.6 μm thick was prepared by spin-coating on the silicon wafer. Then, the functionalized PSU film was mounted onto the thick nf-PSU strip, which had been preheated at 200°C for 24 h in advance. The PSU strip was welded with aPA strip by annealing at 200°C for 15 min.

Sample was placed and fixed by glue on a glass plate. A razor blade of thickness b (0.245 mm) was inserted at the interface between the functionalized PSU and aPA layers until it reached 1 cm from the sample edge. After 24 h, the crack opening length a between the edge of the blade and the crack tip was measured, and then the blade was pushed

[1] Instead of PA6, an amorphous polyamide (Grilamide TR55LX, EMS, Japan; M_n20 K) was used for the adhesion test, because it was very hard to prepare the welded sample with uniform thickness of PA6 layer, owing to the low viscosity of PA6 at welding temperature.

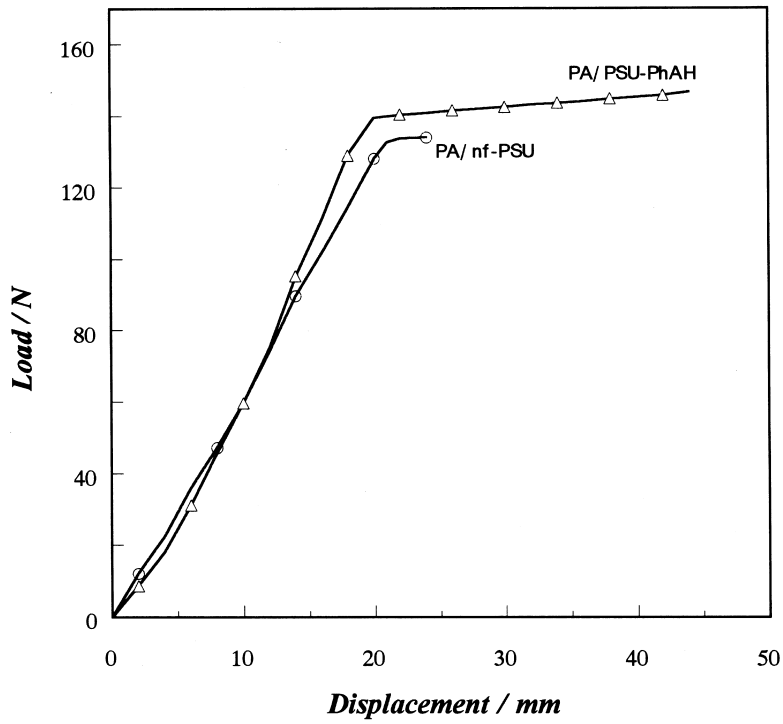

Fig. 8. Typical examples of load-displacement curves of notched specimens tested at cross-head speed of 8 mm min^{-1}: (-○-) PA/nf-PSU and (-△-) PA/PSU-PhAH blends.

in again by 0.5 cm. This procedure was repeated three times and the values were averaged. The fracture toughness, G_c, was then calculated by the following equation [20]:

$$G_c = \frac{3Ed^3b^2}{8a^4[1 + (0.64d/a)]^4}, \quad (4)$$

where E is the Young's modulus of aPA (1.9 GPa) and d is the thickness of upper aPA layer.

4. Results and discussion

TEM micrographs of PA/PSU blends are shown in Fig. 5. Compared with non-reactive system (Fig. 5(a)), the reactive systems yield much smaller particles (Fig. 5(a)–(d)). The results are expected as the reactive systems may generate the PSU-PA graft or block copolymers, which would play a role of an emulsifier to prevent particle coalescence. The calculated average particle diameters from TEM micrographs are listed in Table 2 and shown also in Figs. 7 and 9. Thus, we prepared a series of blend specimens having various particle diameters ranging from 70 nm to 1.3 μm.

Fig. 6(a) shows stress–strain curves of the film specimens of neat PA and neat nf-PSU. As shown, the nf-PSU with low molecular weight is a brittle polymer under the testing condition. It breaks before the yield point. However, PA is a ductile polymer with high elongation at break. Therefore, at 20/80 wt.% (PSU/PA) composition, we are dealing with brittle particles and ductile matrix. Neat functionalized PSUs were also brittle.

A typical stress–strain curve of reactive system, PA/PSU-PhAH, is compared with that of non-reactive system in Fig. 6(b). In a non-reactive system, the ductile behavior of PA is lost by adding 20 wt.% of the brittle PSU, whereas it is preserved in reactive systems. The tensile, mechanical properties of film specimens, elongation at break (E_b) and tensile strength (σ_b) are shown as a function of mean diameter (D_{TEM}) of dispersed PSU particles in Fig. 7. There is a small difference in σ_b among blends. However, the E_b values in the reactive systems are much higher than the non-reactive system. The smaller the PSU particle, the higher is the E_b value.

Fig. 8 shows examples of load-displacement curves of notched specimens at a cross head speed of 8 mm min^{-1}. The bulk fracture toughness may be estimated by the area under the load-displacement curve (A). The reactive system is shown to have wider A than the non-reactive system. As a measure of toughness improvement, A is normalized by $A_{PA/nf\text{-}PSU}$. In Fig. 9 the normalized A is plotted as a function of mean diameter of dispersed PSU particle. For PA/PSU-MAH and PA/PSU-epoxy systems, a moderate toughness improvement, around 30%–40% higher than that of non-reactive system achieved. Remarkable improvement is achieved in PA/PSU-PhAH system having the finest dispersion. The tremendously high toughness at 2 mm min^{-1} may be because of a change in fracture mechanism as will be discussed later.

It is known that toughness improvement depends on several factors such as volume fraction of minor phase, morphology (dispersed particle size, its distribution, or

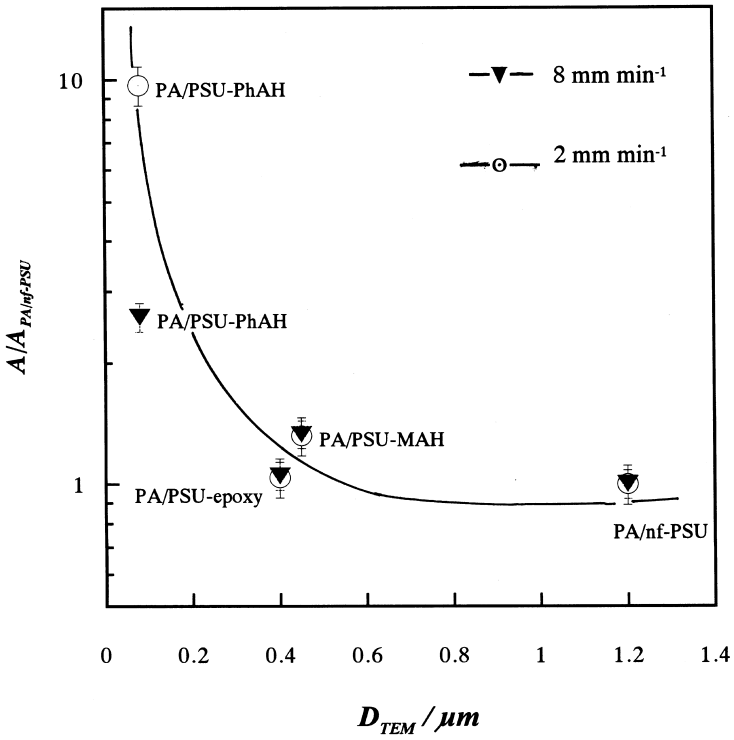

Fig. 9. Mean diameters of dispersed PSU (D_{TEM}) vs. the fracture toughness from area under load-displacement curve of notched specimen, normalized by that of PA/nf-PSU ($A/A_{PA/nf\text{-}PSU}$).

surface-to-surface inter-particle distance), and interfacial adhesion. In the present case, the volume fraction is fixed so that one should discuss whether the toughness improvement is caused by interfacial chemical bonding or simply by the particle size reduction.

Fujita et al. [14] investigated the effect of particle size on the mechanical properties of brittle/ductile blends, PS/PC system. They prepared a series of non-reactive blends with different particle size ranging from 0.3 to 1 μm by adjusting the mixing temperature. They found that there was no dramatic difference in the impact toughness and tensile properties of these blends. Recently, a similar result was also found in non-reactive thermoplastic-rubber blend, PP/NBR by Liu and Baker [23]. Without any interfacial chemical bonding, the impact strength of the blends was hardly improved. The aforementioned results seem to suggest that by only particle size adjustment, the toughness improvement may not be achieved. However, the effect of the particle size might appear on the crystalline structure of PA matrix. Actually, the effect was investigated on the isothermal crystallization at high temperature (T_c = 200°C) by LS, SAXS, WAXD and DSC [18]. It was found that the spherulite with radius of more 10 μm could develop despite the presence of the PSU obstacles. The smaller PSU particle system yielded higher ordering of optical axis within spherulite but less ordering in lamella arrangement and crystal lattice. In contrast, such size effects were never observed for the quenched film specimens as follows.

No visible spherulite was found under the optical microscope in both polarized and unpolarized modes for both neat PA and blends. Four-leaf clover pattern, characteristic pattern of spherulitic nature, did not appear in H_v LS. Scattering intensity at $\mu = 45°$ decreased monotonically with scattering angle as shown in Fig. 10(a). Similar LS profiles were observed in other blends. From the monotonically decreasing LS scattering profiles, the orientation correlation distance ξ_1 was calculated to characterize the crystalline morphology in terms of the degree of correlation in crystallite orientation [24,25]. The results are shown in Table 2. Note that PA-PSU two-phase nature does not affect the values of ξ_1, as they are obtained under H_v mode.

There was also no obvious peak or shoulder corresponding to lamella spacing in SAXS profiles (Fig. 10(b)), suggesting disordered lamellar arrangement. SAXS profiles for other blends were almost the same as Fig. 10(b). From the monotonically decreasing SAXS scattering profiles, the correlation distance in density fluctuation ξ_2 was calculated to describe the length scale of heterogeneity caused by crystallization [26,27] The results are summarized in Table 2. Note that the heterogeneity in PA-PSU two-phase structure is at much longer length scale (μm–sub-μm) so that it hardly affects the values of ξ_2 in 10 nm order.

A diffraction peak at diffraction angle $2\theta = 21.3°$ appeared in WAXD profile as shown in Fig. 10(c). This diffraction peak can be assigned to (0 0 1) reflection from γ crystal [28]. Similar WAXD profiles were observed for other blends. The results of thermal analysis by DSC are also summarized in Table 2. The reactive blends have a

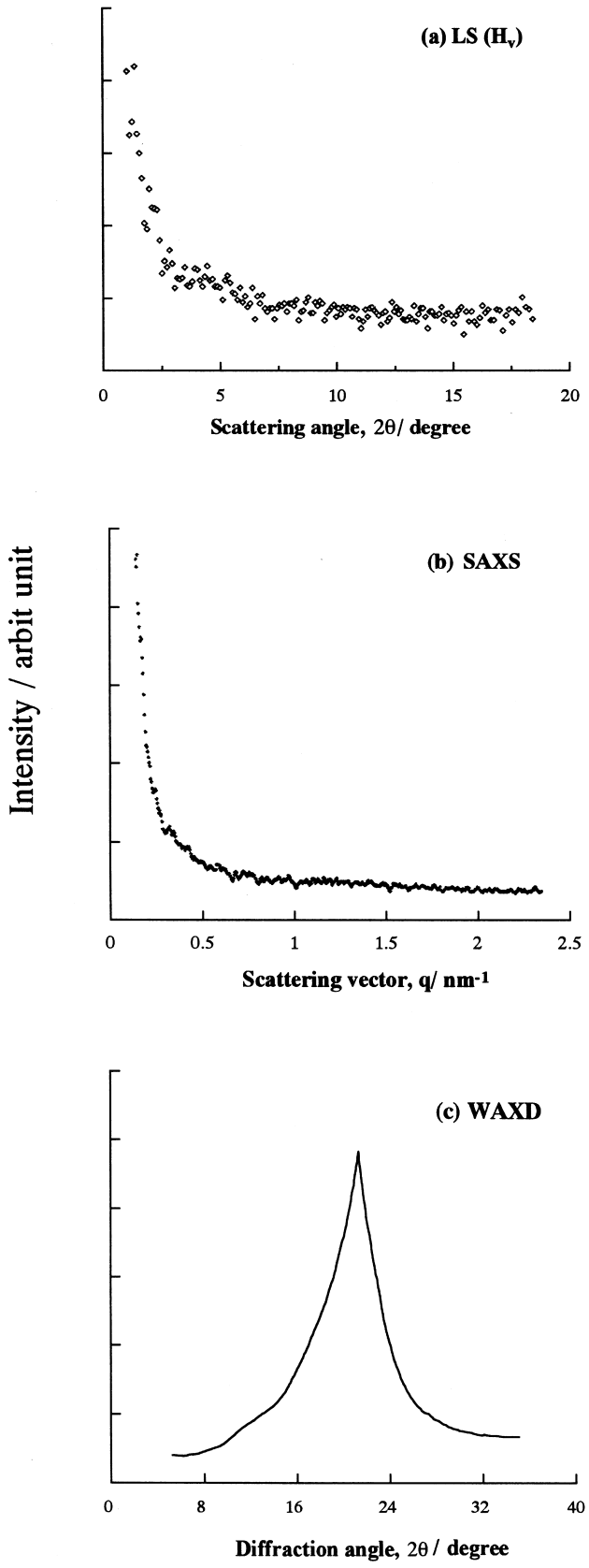

Fig. 10. LS, SAXS and WAXD profiles of PA/PSU-PhAH (quenched film specimen). Scattering vector $q = (4\pi/\lambda)\sin\theta$, λ and θ being wavelength and scattering angle.

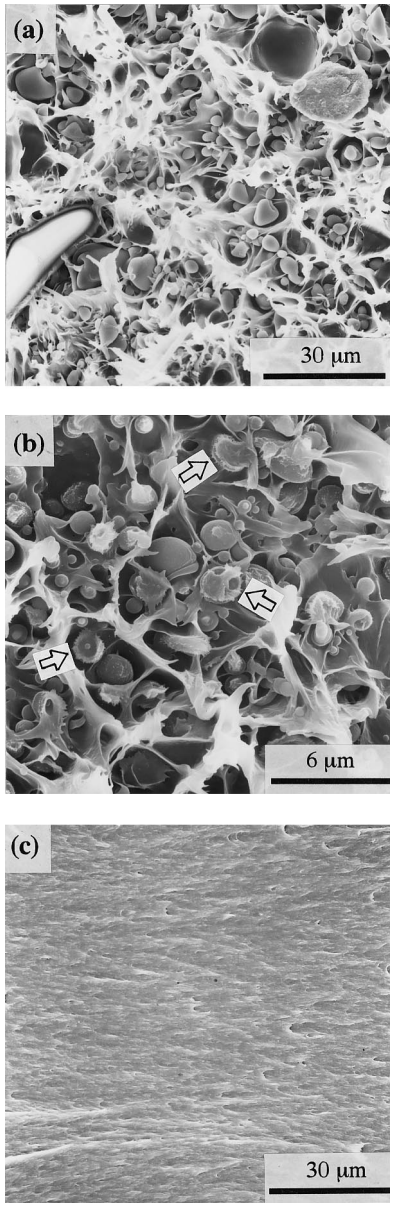

Fig. 11. FE-SEM micrographs of the fractured surface of specimens tested at cross head speed of 2 mm min^{-1}: (a) PA/nf-PSU; (b) PA/PSU-MAH; and (c) PA/PSU-PhAH.

slightly lower melting point and slightly smaller crystallinity than those of the non-reactive system and neat PA. However, the differences are quite small. Thus, the results from LS, SAXS, WAXD and DSC studies lead to a conclusion that there is no significant difference in crystalline morphology among blends;[2] then the difference in mechanical properties may be caused by another reason.

Results of interfacial adhesion in terms of the fracture

[2] At high crystallization temperature (200°C), spherulite could grow up by circumventing the PSU particles and the smaller PSU particles rendered a less ordered lamellar stacking and less perfection of PA crystal [19]. Such effects of PSU particle size seem to be negligibly small for the crystallization by rapid quench in water (present case).

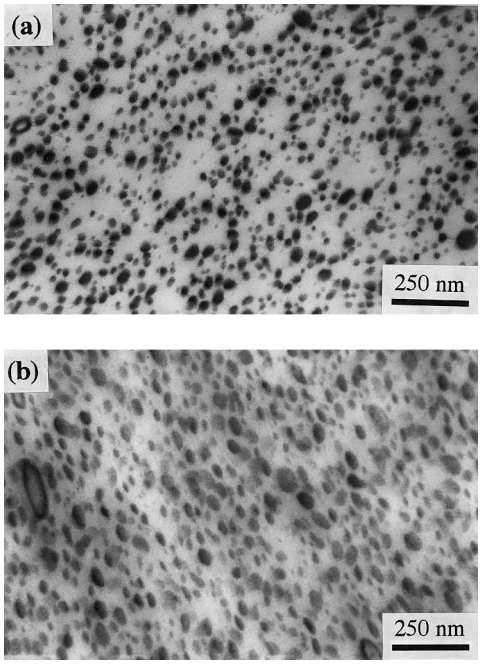

Fig. 12. TEM micrographs of ultrathin section of PA/PSU-PhAH blend after fracture test at cross-speed 2 mm min^{-1}: (a) deformed zone (very near the fractured surface) and (b) 3 mm deep from the fractured surface (see Fig. 3).

toughness G_c by ADCB are also summarized in Table 2. For the non-reactive system, G_c is nearly zero suggesting almost no interfacial adhesion between two phases. All reactive systems show higher G_c values. It is probably caused by the in situ formed graft or block copolymers at the interface. The highest G_c value (120 Jm^{-2}) is obtained for PA/PSU-PhAH system, while 35 and 27 Jm^{-2} for PA/PSU-MAH and PA/PSU-epoxy systems, respectively. One can clearly conclude that higher G_c renders higher toughness of blends. Then, the toughening mechanism in relation to the interfacial adhesion is to be discussed.

Fig. 11 shows typical FE-SEM micrographs of fractured surfaces of notched specimens after testing at cross head rate of 2 mm min^{-1}. For the brittle fracture of PA/nf-PSU, debonding between matrix PA and dispersed particle is clearly seen, suggesting very weak interfacial adhesion (Fig. 11(a)). The situation seems to be similar for PA/PSU-MAH blend (Fig. 11(b)). However, one could clearly see short fibrils on several PSU particles as indicated by arrows. This may be because of the interfacial activity of in situ formed PA-PSU graft copolymers, which increase adhesion strength between the dispersed and the matrix phases. Enhancement of interfacial adhesive strength may be responsible for 30%–40% toughness improvement (Fig. 9). Fig. 11(c) represents the fractured surface of PA/PSU-PhAH. In this case, the micrograph shows no evidence of interfacial de-bonding or cavitation even at higher magnification (not shown here). Whole material including fine PSU particles seems to have plastically deformed. That is, the two-phase material seems to be homogeneously yielded without debonding. If so, the brittle PSU particles are expected to be elongated perpendicular to the fracture surface. Fig. 12 shows TEM micrographs of ultrathin sections of PA/PSU-PhAH cut in perpendicular to loading direction. The locations of sectioning for Fig. 12(a) and (b) are in the deformed zone (very near to fractured surface) and far from deformed zone (3 mm from fractured surface), respectively. From the micrographs, one can see that the average PSU particle size in the deformed zone (56 nm) is slightly smaller than that of the undeformed zone (65 nm). The former may correspond to short semi-axis of deformed PSU ellipse and the latter to the undeformed particle diameter, suggesting a definite deformation of the brittle PSU particles.

5. Conclusion

Morphology-interface-toughness relationships of brittle dispersed PSU in ductile PA matrix blends prepared by reactive blending were investigated. Significant toughness improvement was found in PA/PSU-PhAH system with finest morphology. Moderate improvement was achieved in other reactive systems. High toughness in PSU-PhAH blend seems to originate from the enhanced interfacial adhesion, which provide adequate stress transfer to induce the cold drawing of brittle PSU particles.

Acknowledgements

The authors acknowledge the German Government, BMBF, for providing them a research fund (Project 03 N30283). We also thank Dr. S. Asai, TIT, for helping with the SAXS experiments.

References

[1] Wu S. J Polym Sci Polym Phys Ed 1983;21:699.
[2] Wu S. Polymer 1985;26:1855.
[3] Borggreve RJM, Gaymans RJ, Eichenwald HM. Polymer 1989;30:78.
[4] Hobbs SY, Dekkers MEJ. J Mater Sci 1989;24:1316.
[5] Sue HJ, Yee AF. J Mater Sci 1991;26:3449.
[6] Fukui T, Kikuchi Y, Inoue T. Polymer 1991;32:2367.
[7] Koo K, Inoue T, Miyasaka K. Polym Eng Sci 1985;25:741.
[8] Karauchi T, Ohta T. J Mater Sci 1984;19:1669.
[9] Angola JC, Fujita Y, Sakai T, Inoue T. J Polym Sci: Polym Phys Ed 1988;26:807.
[10] Liu TM, Xie HQ, O'Callaghan KJ, Rudin A, Baker WE. J Polym Sci: Polym Phys Ed 1993;31:1347.
[11] Evans RD, MacGillivray LA, Boyd JD, Baker WE, Pith T. Polym Net Blds 1996;6:81.
[12] Ibuki J, Charoensirisomboon P, Chiba T, Ougizawa T, Inoue T, Weber M, Koch E. Polymer 1999;40:647.
[13] Charoensirisomboon P, Solomko SI, Inoue T, Weber M. Polym Prep Jpn 1998;47:2718.
[14] Fujita Y, Koo K, Angola JC, Sakai T. Inoue. T. Kobunshi Ronbushu 1986;43:119.
[15] Esser ICHM, Parsons IA. Polymer 1993;34:1836.

[16] Koch H, Ritter H. Makromol Chem Phys 1994;195:1709.
[17] D.E.-A 41 10 460 BASF-AG.
[18] Lee CH, Saito H, Inoue T. Macromolecules 1993;26:6566.
[19] Charoensirisomboon P, Saito H, Inoue T, Weber M. Macromolecules 1998;31:4963.
[20] Dole M, Wunderlich BB. Macromol Chem 1959;34:29.
[21] Kanninen MF. Int J Fract 1973;9:83.
[22] Brown HR. J Mater Sci 1990;25:2791.
[23] Liu NC, Baker WE. Polymer 1994;35:988.
[24] Stein RS, Wilson PR. J Appl Phys 1962;33:1914.
[25] Stein RS, Stidham SN. J Appl Phys 1964;35:42.
[26] Debye P, Bueche AM. J Appl Phys 1949;20:518.
[27] Debye P, Anderson HR, Brumberger H. J Appl Phys 1957;28:679.
[28] Holms DR, Bunn CW, Smith DJ. J Polym Sci 1955;27:159.